EPJ manuscript No.
(will be inserted by the editor)

Magnetic properties of the quantum spin-$\frac{1}{2}$ XX diamond chain: The Jordan-Wigner approach

Taras Verkholyak[1,2], Jozef Strečka[2], Michal Jaščur[2], Johannes Richter[3]

[1] Institute for Condensed Matter Physics, National Academy of Sciences of Ukraine, 1 Svientsitskii Street, L'viv-11, 79011, Ukraine
[2] Department of Theoretical Physics and Astrophysics, Institute of Physics, P. J. Šafárik University, Park Angelinum 9, 040 01 Košice, Slovak Republic
[3] Institut für Theoretische Physik, Otto-von-Guericke-Universität Magdeburg, P.O. Box 4120, 39016 Magdeburg, Germany

Received: date / Revised version: date

Abstract. The Jordan-Wigner transformation is applied to study magnetic properties of the quantum spin-$\frac{1}{2}$ XX model on the diamond chain. Generally, the Hamiltonian of this quantum spin system can be represented in terms of spinless fermions in the presence of a gauge field and different gauge-invariant ways of assigning the spin-fermion transformation are considered. Additionally, we analyze general properties of a free-fermion chain, where all gauge terms are neglected and discuss their relevance for the quantum spin system. A consideration of interaction terms in the fermionic Hamiltonian rests upon the Hartree-Fock procedure after fixing the appropriate gauge. Finally, we discuss the magnetic properties of this quantum spin model at zero as well as non-zero temperatures and analyze the validity of the approximation used through a comparison with the results of the exact diagonalization method for finite (up to 36 spins) chains. Besides the $m = 1/3$ plateau the most prominent feature of the magnetization curve is a jump at intermediate field present for certain values of the frustrating vertical bond.

PACS. XX.XX.XX No PACS code given

1 Introduction

Low-dimensional quantum spin models on frustrated lattices represent objects of intense current research (see e.g. Refs.[1,2,3,4] for the recent reviews). The analytical study of such models is however quite involved, since the interplay of competing interactions, quantum fluctuations and magnetic field may produce at sufficiently low temperatures a diversity of unusual quantum phases. A dimerization in the ground state, localized excitations, magnetization jumps and plateaus are the most typical phenomena, which might possibly appear in geometrically frustrated quantum spin models[1,2,3,4,5,6].

The spin-$\frac{1}{2}$ Heisenberg model on the diamond chain is an example of a frustrated spin system, which represents one of the simplest quantum models with the exactly known monomer-dimer ground state. When the nearest-neighbor spins from a diamond chain are coupled through antiferromagnetic interactions, this model actually exhibits either ferrimagnetically ordered ground states or the disordered tetramer-dimer and dimer-monomer spin-fluid phases depending on the relative strength of the geometric frustration [7]. A number of exact results for low-temperature properties are also available at sufficiently high magnetic fields close to a saturation value at which this quantum system shows a magnetization jump towards the completely polarized phase (see e.g. Refs. [4,5] and [6]). Exact results can be also found for the special Ising-Heisenberg diamond chain when the only quantum interaction is between spins on vertical bonds and one may apply the decoration-iteration transformation to study this simplified model rigorously in the whole temperature range [8]. Most recently the ground states of the mixed diamond chain with higher spins have been found rigorously [9]. Quantum phase transitions and finite-temperature properties of the diamond chain with the mixed spins 1 and 1/2 have been studied in Refs.[10,11].

The ground-state phase diagram of the spin-$\frac{1}{2}$ Heisenberg model on the distorted diamond chain cannot be found exactly in general, but the extensive study of the ground phase has been performed in Refs. [12,13] by means of the exact diagonalization and some perturbative approaches. The effect of the exchange anisotropy on the ground state properties of the spin-$\frac{1}{2}$ XXZ diamond chain was considered in Refs. [14,15,16], where the interesting inversion phenomenon has been theoretically predicted. In the case of the easy-plane anisotropy, the ground-state phase diagram contains an additional Néel phase as a result of the interplay between the exchange anisotropy, geometric frustration and quantum fluctuations.

The experimental detection of the frustrated diamond chain in azurite $Cu_3(CO_3)_2(OH)_2$ [17], the ferrimagnetic diamond chain in organic-radical system [18], as well as, the ferromagnetic diamond chains in polymeric coordination compounds $Bi_4Cu_3V_2O_{14}$ [19], $Cu_3(TeO_3)_2Br_2$ [20] and $Cu_3(N_3)_6(DMF)_2$ [21] have stimulated a number of experimental [22,23,24,25,26,27] and theoretical [8,28,29, 30,31] studies over the last few years. The study of the field-dependent magnetization curve in the ground state, dynamic properties and the determination of spin couplings are the most discussed problems nowadays [27,28, 30,31].

Most of the previous theoretical treatments are based on numerical techniques. Hence an analytical approach covering the ground state as well as thermodynamic properties is desirable. A promising method is the Jordan-Wigner fermionization of the spin degrees of freedom. Such an approach has been presented in Refs. [29,30]. However, the results presented there suffer from the neglecting of phase factors and, therefore, they cannot be considered as reliable (see our discussion in Sect. 3). Note that the Jordan-Wigner transformation also gives a useful representation for the quantum models on two-leg ladders [32, 33,34]. In the case of the railroad ladder approximative considerations allow to describe not only the ground state, but also the dynamic properties [33].

The goal of the present paper is to describe thermodynamic and magnetic properties of the quantum spin-$\frac{1}{2}$ XX diamond chain in fermionic language by means of the Jordan-Wigner transformation and to complement our findings by exact diagonalization data. It should be stressed, however, that the diamond chain model is not reduced after performing the Jordan-Wigner transformation to free fermions. The XX interaction terms are not mapped to the two-fermion terms but they might contain phase factors whose specific form will basically depend on a particular choice of the nonlocal Jordan-Wigner transformation (see the discussion on the railroad ladder in Ref. [33]). On the other hand, all different fermionic representations are connected through appropriate gauge transformations. Because of the phase factors, which effectively introduce interactions between fermions and act as operators, the quantum diamond chain model cannot be treated rigorously anymore and some further approximations are required. Note that this kind of fermionic representation is extremely useful for studying dynamic properties of quantum spin-$\frac{1}{2}$ models (see e.g. Refs. [35, 36]).

The outline of this paper is as follows. In Sec. 2, the Jordan-Wigner transformation for the spin-$\frac{1}{2}$ XX model on the diamond chain will be considered. The free-fermion model and its relation to the quantum spin model is analyzed in Sec. 3. The Hartree-Fock approximation is applied to the fermionic counterpart of the symmetric and distorted diamond chain in Secs. 4 and 5. The ground-state properties will be finally calculated and compared with the known exact and numerical results there. The thermodynamic properties will be considered in Sec. 6 and the obtained results are summarized in Sec. 7.

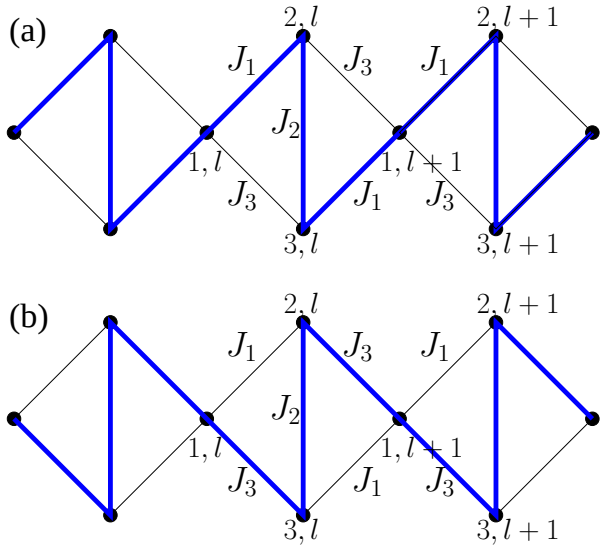

Fig. 1. Different ways of assigning Jordan-Wigner transformation on the diamond chain are marked by thick lines. The case **i)** (panel a) and the case **ii)** (panel b), see the main text.

2 Jordan-Wigner transformation for the spin-$\frac{1}{2}$ XX diamond chain

Consider the quantum spin-$\frac{1}{2}$ XX model on the diamond chain (see Fig. 1) with the following Hamiltonian:

$$H_{xx} = \frac{1}{2}\sum_{l=1}^{N}\Big[(J_2 s^+_{2,l}s^-_{3,l} + J_1(s^+_{1,l}s^-_{2,l} + s^+_{3,l}s^-_{1,l+1}) + J_3(s^+_{1,l}s^-_{3,l} + s^+_{2,l}s^-_{1,l+1}) + \text{h.c.}) - 2h\sum_{p=1}^{3}\left(s^+_{p,l}s^-_{p,l} - \frac{1}{2}\right)\Big]. \quad (1)$$

Here, N is the number of unit cells, $s^{\pm}_{p,l} = s^x_{p,l} \pm i s^y_{p,l}$ are the spin raising and lowering operators, $s^z_{p,l} = s^+_{p,l}s^-_{p,l} - \frac{1}{2}$, $s^{\alpha}_{m,l}$ ($\alpha = x, y, z$) are the usual Cartesian components of the Pauli spin-$\frac{1}{2}$ operator with the first index corresponding to a sublattice and the second to a cell. h is the external magnetic field (we set $g\mu_B = 1$). We will further distinguish between two models: the distorted ($J_1 \neq J_3$) and the symmetric ($J_1 = J_3$) diamond chain.

The Jordan-Wigner transformation can be unambiguously defined on a linear chain [37,38], where all sites can be enumerated subsequently. The diamond chain is however a three sublattice model and there exists at least two identical ways of arranging its sites in a one-dimensional sequence as shown on panels (a) and (b) in Fig. 1. The case **i)** sets the following order of sites $\ldots, (3, l-1), (1, l), (2, l), (3, l), (1, l+1), \ldots$ and the case **ii)** corresponds to another choice of order $\ldots, (2, l-1), (1, l), (3, l), (2, l), (1, l+1), \ldots$.

Following the usual procedure one can define the nonlocal Jordan-Wigner transformation, which introduces new

Fermi operators by multiplying the spin lowering and raising operators by the Jordan-Wigner factors $(-2s^z_{l,m})$ referring to all preceding spins [37,38]. For the case **i)** we have:

$$
\begin{aligned}
s^-_{1,l}&=a_{1,l}\exp\left[-i\pi\sum_{p=1}^{3}\sum_{i=1}^{l-1}a^+_{p,i}a_{p,i}\right],\\
s^-_{2,l}&=a_{2,l}\exp\left[-i\pi\left(a^+_{1,l}a_{1,l}+\sum_{p=1}^{3}\sum_{i=1}^{l-1}a^+_{p,i}a_{p,i}\right)\right],\\
s^-_{3,l}&=a_{3,l}\exp\left[-i\pi\left(a^+_{1,l}a_{1,l}+a^+_{2,l}a_{2,l}+\sum_{p=1}^{3}\sum_{i=1}^{l-1}a^+_{p,i}a_{p,i}\right)\right],\\
s^z_{n,l}&=s^+_{n,l}s^-_{n,l}-\frac{1}{2}=a^+_{n,l}a_{n,l}-\frac{1}{2}.
\end{aligned}
\tag{2}
$$

Subsequently, the spin interaction terms to emerge in the Hamiltonian (1) can also be rewritten by the use of Eqs. (2) into the fermionic representation: $s^+_{1,l}s^-_{2,l}=a^+_{1,l}a_{2,l}$, $s^+_{2,l}s^-_{3,l}=a^+_{2,l}a_{3,l}$, $s^+_{1,l}s^-_{3,l}=a^+_{1,l}\mathrm{e}^{i\pi a^+_{2,l}a_{2,l}}a_{3,l}$, $s^+_{2,l}s^-_{1,l+1}=a^+_{2,l}\mathrm{e}^{i\pi a^+_{3,l}a_{3,l}}a_{1,l+1}$, $s^+_{3,l}s^-_{1,l+1}=a^+_{3,l}a_{1,l+1}$. Hence, it follows that the fermionic representation of the Hamiltonian of the spin-$\frac{1}{2}$ XX diamond chain then reads:

$$
\begin{aligned}
H_{xx}=\ &\frac{1}{2}\sum_{l=1}^{N}\Big[(J_2a^+_{2,l}a_{3,l}+J_1(a^+_{1,l}a_{2,l}+a^+_{3,l}a_{1,l+1})\\
&+J_3(a^+_{1,l}\mathrm{e}^{i\pi a^+_{2,l}a_{2,l}}a_{3,l}+a^+_{2,l}\mathrm{e}^{i\pi a^+_{3,l}a_{3,l}}a_{1,l+1})\\
&+\text{h.c.})-2h\sum_{p=1}^{3}\left(a^+_{p,l}a_{p,l}-\frac{1}{2}\right)\Big].
\end{aligned}
\tag{3}
$$

In the current ordering the sites $(1,l)$, $(3,l)$ and $(2,l)$, $(1,l+1)$ are not nearest neighbors. Therefore, the corresponding couplings contain phase factors in the hopping terms that prevent a rigorous consideration of the investigated model. By imposing periodic boundary conditions in the considered model $s^{\pm}_{N,l}s^{\mp}_{1,m}$ transform into many fermion terms. Such boundary terms may be neglected after making the Jordan-Wigner transformation, since they are irrelevant for the study of static properties in the thermodynamic limit [37,38].

Considering the numbering of sites **ii)** the Jordan-Wigner transformation should be defined as:

$$
\begin{aligned}
s^-_{1,l}&=\tilde{a}_{1,l}\exp\left[-i\pi\sum_{p=1}^{3}\sum_{i=1}^{l-1}\tilde{a}^+_{p,i}\tilde{a}_{p,i}\right],\\
s^-_{2,l}&=\tilde{a}_{2,l}\exp\left[-i\pi\left(\tilde{a}^+_{1,l}\tilde{a}_{1,l}+\tilde{a}^+_{3,l}\tilde{a}_{3,l}+\sum_{p=1}^{3}\sum_{i=1}^{l-1}\tilde{a}^+_{p,i}\tilde{a}_{p,i}\right)\right],\\
s^-_{3,l}&=\tilde{a}_{3,l}\exp\left[-i\pi\left(\tilde{a}^+_{1,l}\tilde{a}_{1,l}+\sum_{p=1}^{3}\sum_{i=1}^{l-1}\tilde{a}^+_{p,i}\tilde{a}_{p,i}\right)\right].
\end{aligned}
\tag{4}
$$

Hence, one gets another fermionic representation of the original Hamiltonian (1):

$$
\begin{aligned}
H_{xx}=\ &\frac{1}{2}\sum_{l=1}^{N}\Big[(J_2\tilde{a}^+_{2,l}\tilde{a}_{3,l}+J_3(\tilde{a}^+_{1,l}\tilde{a}_{3,l}+\tilde{a}^+_{2,l}\tilde{a}_{1,l+1})\\
&+J_1(\tilde{a}^+_{1,l}\mathrm{e}^{i\pi\tilde{a}^+_{3,l}\tilde{a}_{3,l}}\tilde{a}_{2,l}+\tilde{a}^+_{3,l}\mathrm{e}^{i\pi\tilde{a}^+_{2,l}\tilde{a}_{2,l}}\tilde{a}_{1,l+1})\\
&+\text{h.c.})-2h\sum_{p=1}^{3}\left(\tilde{a}^+_{p,l}\tilde{a}_{p,l}-\frac{1}{2}\right)\Big].
\end{aligned}
\tag{5}
$$

It should be noted that the Hamiltonian (5) differs from the Hamiltonian (3). The hopping terms, which have not contained the fermion interaction before, now acquire a phase factor, and conversely, in other terms the relevant phase factors have disappeared. A common feature of both Hamiltonians is that they contain the interaction only at some particular bonds, and therefore, if one intends to treat the model approximatively, the contributions of different bonds will not be generally considered on equal footing.

Using (2), (4) one can check that operators $a_{p,m}$ and $\tilde{a}_{p,m}$ are connected through the gauge transformation:

$$
\begin{aligned}
&a_{1,l}=\tilde{a}_{1,l},\\
&a_{2,l}=\tilde{a}_{2,l}\exp\left(i\pi\tilde{a}^+_{3,l}\tilde{a}_{3,l}\right),\ \tilde{a}_{2,l}=a_{2,l}\exp\left(i\pi a^+_{3,l}a_{3,l}\right),\\
&a_{3,l}=\tilde{a}_{3,l}\exp\left(i\pi\tilde{a}^+_{2,l}\tilde{a}_{2,l}\right),\ \tilde{a}_{3,l}=a_{3,l}\exp\left(i\pi a^+_{2,l}a_{2,l}\right).
\end{aligned}
\tag{6}
$$

Thus, the Hamiltonians (3) and (5) describe the same physics.

One can also consider a more general gauge transformation for Fermi operators c_x:

$$
\tilde{c}_x=\mathrm{e}^{i\sum_{y\neq x}\alpha_{xy}n_y}c_x,
\tag{7}
$$

where x, y are general indices which may include the site and sublattice numbers. If $\alpha_{xy}=\alpha_{yx}+2\pi n$ new operators $\tilde{c}_x$ satisfy the Fermi commutation relations.

Fixing the gauge in transformation (7), we can consider a particular case:

$$
\begin{aligned}
&c_{1,l}=a_{1,l},\\
&c_{2,l}=\mathrm{e}^{i\frac{\pi}{2}a^+_{3,l}a_{3,l}}a_{2,l},\ a_{2,l}=\mathrm{e}^{-i\frac{\pi}{2}c^+_{3,l}c_{3,l}}c_{2,l},\\
&c_{3,l}=\mathrm{e}^{i\frac{\pi}{2}a^+_{2,l}a_{2,l}}a_{3,l},\ a_{3,l}=\mathrm{e}^{-i\frac{\pi}{2}c^+_{2,l}c_{2,l}}c_{3,l}.
\end{aligned}
\tag{8}
$$

This gives as a result the Hamiltonian in the most symmetric form:

$$
\begin{aligned}
H_{xx}=\ &\frac{1}{2}\sum_{l=1}^{N}\Big[(J_1(c^+_{1,l}\mathrm{e}^{-i\frac{\pi}{2}c^+_{3,l}c_{3,l}}c_{2,l}+c^+_{3,l}\mathrm{e}^{i\frac{\pi}{2}c^+_{2,l}c_{2,l}}c_{1,l+1})\\
&+J_3(c^+_{1,l}\mathrm{e}^{i\frac{\pi}{2}c^+_{2,l}c_{2,l}}c_{3,l}+c^+_{2,l}\mathrm{e}^{-i\frac{\pi}{2}c^+_{3,l}c_{3,l}}c_{1,l+1})\\
&+J_2c^+_{2,l}c_{3,l}+\text{h.c.})-2h\sum_{p=1}^{3}\left(c^+_{p,l}c_{p,l}-\frac{1}{2}\right)\Big].
\end{aligned}
\tag{9}
$$

One can also easily find the spin-fermion transformation that leads to the representation (8). It takes the form:

$$s^-_{1,l}=c_{1,l}\exp\left[-i\pi\sum_{p=1}^{3}\sum_{i=1}^{l-1}c^+_{p,i}c_{p,i}\right], \quad (10)$$

$$s^-_{2,l}=c_{2,l}\exp\left[-i\pi\left(\frac{1}{2}c^+_{3,l}c_{3,l}+c^+_{1,l}c_{1,l}+\sum_{p=1}^{3}\sum_{i=1}^{l-1}c^+_{p,i}c_{p,i}\right)\right],$$

$$s^-_{3,l}=c_{3,l}\exp\left[-i\pi\left(-\frac{1}{2}c^+_{2,l}c_{2,l}+c^+_{1,l}c_{1,l}+\sum_{p=1}^{3}\sum_{i=1}^{l-1}c^+_{p,i}c_{p,i}\right)\right].$$

Finally, one should note that equations (10) represent a more general formulation of the Jordan-Wigner transformation for the spin ladders:

$$s^+_x = c^+_x \mathrm{e}^{i\pi\phi_x}, \phi_x = \sum_{y\neq x}\varphi_{x,y}c^+_y c_y \quad (11)$$

with the condition $\varphi_{x,y} = \varphi_{y,x} \pm 1$ [33]. Here x, y are again general indices which may include the site and sublattice numbers.

We would like also to comment some limiting cases of the model. If $J_1 = 0$ or $J_3 = 0$ the model resembles the exactly solvable trimerized XX chain [39,40,41]. Indeed, if $J_3 = 0$ (or $J_1 = 0$) we come after the Jordan-Wigner transformation (2) (or (4)) to the Hamiltonian (3) (or (5)) in the form of free fermions. In case $J_2 = 0$ but $J_1 \neq 0$, $J_3 \neq 0$ it is not possible to find such a form of the Jordan-Wigner transformation that avoids the interaction between fermions in the transformed Hamiltonian. Therefore, the consideration of the models with $J_1 \neq 0$, $J_3 \neq 0$ requires further approximations even if $J_2 = 0$.

For the further consideration it is useful to remind that the $|\downarrow\rangle_n$ ($|\uparrow\rangle_n$) spin state corresponds to the empty $|0\rangle_n$ (filled $|1\rangle_n = c^+_n|0\rangle_n$) fermion state. Thus, the magnetization per spin in z-direction is related to the fermionic averages in the following way:

$$m_z=\frac{1}{3N}\sum_{p=1}^{3}\sum_{l=1}^{N}\left\langle s^z_{p,l}\right\rangle=\frac{1}{3N}\sum_{p=1}^{3}\sum_{l=1}^{N}\left\langle c^+_{p,l}c_{p,l}\right\rangle-\frac{1}{2}. \quad (12)$$

3 Phase factors and their importance. Free-fermion model on diamond chain

Now we would like to analyze the general properties of the free-fermion model on the diamond chain, i.e., the model which one gets after the Jordan-Wigner transformation ignoring the phase factors terms [29].

The Hamiltonian of the spin-$\frac{1}{2}$ XX model, as well as a more general XXZ model, in zero field is invariant under the reflection of z-component of all spins: $s^z_{p,l} \to -s^z_{p,l}$ [$|\uparrow\rangle_{p,l} \to |\downarrow\rangle_{p,l}$]. In fermionic language it corresponds to the particle-hole transformation: $a_{p,l} \to a^+_{p,l}$ [$|0\rangle_{p,l} \to |1\rangle_{p,l}$]. It is clear that the Hamiltonian of the free-fermion gas is not invariant under such transformation because all the terms change their signs:

$$H_{ff} = -\frac{1}{2}\sum_{l=1}^{N}\Big(J_2 a^+_{2,l}a_{3,l} + J_1(a^+_{1,l}a_{2,l} + a^+_{3,l}a_{1,l+1}) + J_3(a^+_{1,l}a_{3,l} + a^+_{2,l}a_{1,l+1}) + \text{h.c.}\Big). \quad (13)$$

One may also use a kind of phase transformation ($\tilde{a}_{p,l} = (-1)a_{p,l}$) for some sites to revert the signs. However, five terms of the Hamiltonian (13) should reverse their signs for every particular l using transformations for only three operators and hence it follows that it is impossible to satisfy simultaneously all the conditions quite generally. However, such a possibility appears for some particular cases $J_1 = 0$ or $J_3 = 0$ which correspond to the exactly solvable trimerized chain [39,40,41]. The situation for the Hamiltonians (3) and (5) is different. After the particle-hole transformation the terms which contain phase factors preserve their signs, the signs of other two-fermionic terms can be always reverted by the aforementioned phase transformations.

Thus, the symmetry of the spin-$\frac{1}{2}$ model is broken in the free-fermion Hamiltonian. It may mean that the magnetization calculated from this Hamiltonian is not an odd function of the external magnetic field anymore. We can prove it in a way similar to [42]. One has to calculate the magnetization using the fermionic representation:

$$m_z=\frac{1}{3N}\sum_{p=1}^{3}\sum_{i=1}^{N}\langle s^z_{p,i}\rangle=-\frac{1}{2}\int\limits_{-\infty}^{\infty}dE\rho(E)\tanh\left(\frac{\beta E}{2}\right) \quad (14)$$

where $\beta = 1/T$ is the inverse temperature. We have also introduced the density of states

$$\rho(E) = \frac{1}{3N}\sum_{p=1}^{3}\sum_{i=1}^{N}\delta(E - \Lambda_{p,i}). \quad (15)$$

$\Lambda_{p,i}$ denote the eigenvalues of the free-fermion Hamiltonian (13). Generally, one has to prove the asymmetry of the density of states for $h = 0$. The simplest way is to show that the odd moments for the density of states

$$M^{(l)} = \int_{-\infty}^{\infty}dE E^l\rho(E)$$

can take non-zero values. Using the Green's function method [43], we find the third moment in the form:

$$M^{(3)} = -h^3 - \frac{1}{2}h(J_2^2+2J_1^2+2J_3^2) + \frac{1}{2}J_1J_2J_3. \quad (16)$$

Hence, it remains nonzero in the zero-field case and gives a nonzero contribution to the zero-field magnetization.

This general conclusion can be confirmed by numerical calculations. The free-fermion Hamiltonian (13) can be diagonalized by subsequent application of the Fourier transformation (which present the Hamiltonian as a 3×3

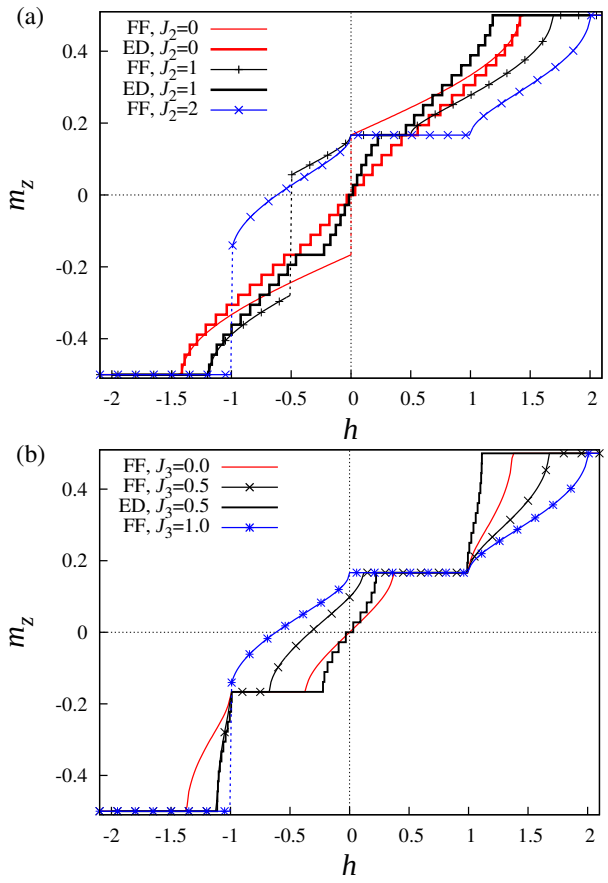

Fig. 2. (Color online) The ground-state magnetization vs. the external field of the free-fermion (FF) model on: a) the symmetric diamond chain $J_1 = J_3 = 1$, $J_2 = 0, 1, 2$, the thick step-like lines correspond to the exact diagonalization (ED) of the spin model (1) of 36 spins for $J_2 = 0, 1$; b) the distorted diamond chain $J_2 = 2$, $J_1 = 1$, $J_3 = 0, 0.5, 1$, the thick step-like line corresponds to the exact diagonalization of the spin model of 36 spins (1) for $J_3 = 0.5$.

quadratic form) and unitary transformation. The eigenenergies $\Lambda_n(\kappa) = h + \omega_n(\kappa)$ are expressed through the solutions $\omega_n(\kappa)$ of the cubic equation:

$$\omega_n(\kappa)^3 + p(\kappa)\omega_n(\kappa) + q(\kappa) = 0,$$
$$p(\kappa) = -\frac{J_2^2}{4} - \frac{J_1^2}{2} - \frac{J_3^2}{2} - J_1 J_3 \cos\kappa,$$
$$q(\kappa) = -\frac{J_2}{4}(2J_1 J_3 + (J_1^2 + J_3^2)\cos\kappa).$$

Here κ is the wave vector of the Fourier transformation, and n is the sublattice index. The density of states is rewritten as $\rho(E) = \sum_n \rho_n(E)$ where $\rho_n(E) = \sum_\kappa \delta(E - h - \omega_n(\kappa))$. Using this representation of the density of states and the expression for the magnetization (14) one can easily understand the curves shown in Fig. 2. The gap between nearest bands corresponds to the plateau of the magnetization. The jumps of the magnetization is a mark of the flat band in the model. Indeed, for the symmetric chain one can find the solution in simple form: $\omega_1(\kappa) = -J_2/2$, $\omega_{2,3}(\kappa) = J_2(1 \pm \sqrt{1 + (4J_1/J_2)^2(1 + \cos\kappa)})/4$. Thus, the ground-state magnetization has the jump at $h = -J_2/2$. Note that in case all couplings J_p are nonzero, the magnetization gains a finite value even for zero fields (see Fig. 2), which is clearly an artifact of the used free-fermion approximation. In Fig. 2 we also compare the magnetization derived from the free-fermion model (13) with the exact diagonalization data of model (1). One can see that the good agreement is achieved for the strong negative fields only where the system is close to the ordered state with all spins down.

To conclude, the free-fermion model on the diamond chain generally looses the symmetry of the corresponding quantum spin model and, moreover, it gives physically not acceptable solution for the nonzero magnetization even in the zero-field case.

4 Hartree-Fock approximation for the distorted diamond chain

When the sites $(2, l)$ and $(3, l)$ are shifted from its symmetric positions, we come to a distorted diamond chain where only some of the spin interactions differ from each other. Without loss of the generality one may impose that $J_1 > J_3$ and choose such a fermionic representation of the Hamiltonian (3) that the fermion interaction terms will finally appear along the weaker bonds only. The latter terms can be then treated perturbatively. Using the algebra of Fermi operators, i.e., $\exp(i\pi a^+_{p,l}a_{p,l}) = 1 - 2a^+_{p,l}a_{p,l}$, one can rewrite (3) in the following form:

$$H_{xx} = \frac{1}{2}\sum_{l=1}^{N}\Big[(J_2 a^+_{2,l}a_{3,l} + J_1(a^+_{1,l}a_{2,l} + a^+_{3,l}a_{1,l+1}) + J_3(a^+_{1,l}(1-2a^+_{2,l}a_{2,l})a_{3,l} + a^+_{2,l}(1-2a^+_{3,l}a_{3,l})a_{1,l+1}) + \text{h.c.}) - 2h\sum_{p=1}^{3}\left(a^+_{p,l}a_{p,l} - \frac{1}{2}\right)\Big]. \quad (17)$$

Applying the Hartree-Fock or mean-field-like approximation [44,45,46] which preserves the correlations between neighboring sites, e.g.

$$a^+_{1,l}a^+_{3,l}a_{3,l}a_{2,l} \approx -a^+_{1,l}a_{3,l}A_1 - A_3 a^+_{3,l}a_{2,l} + A_3A_1 + a^+_{1,l}a_{2,l}\overline{n}_2 + A_2 a^+_{3,l}a_{3,l} - A_2\overline{n}_2, \quad (18)$$

we come to the quadratic form in Fermi operators:

$$H_{xx} \approx \frac{1}{2}\sum_{l=1}^{N}\Big[\big((J_2 + 4J_3A_2)a^+_{2,l}a_{3,l} + (J_1 + 2J_3A_1)(a^+_{1,l}a_{2,l} + a^+_{3,l}a_{1,l+1}) + J_3(1 - 2\overline{n}_2)(a^+_{1,l}a_{3,l} + a^+_{2,l}a_{1,l+1}) + \text{h.c.}\big) - 2ha^+_{1,l}a_{1,l} - 2(h + J_3A_3)(a^+_{2,l}a_{2,l} + a^+_{3,l}a_{3,l})\Big] + Ne_0. \quad (19)$$

Here we use the following notations: $A_1 = \langle a^+_{2,l} a_{3,l}\rangle$, $A_2 = \langle a^+_{1,l} a_{2,l}\rangle = \langle a^+_{3,l} a_{1,l+1}\rangle$, $A_3 = \langle a^+_{1,l} a_{3,l}\rangle = \langle a^+_{2,l} a_{1,l+1}\rangle$, $\overline{n}_2 = \langle a^+_{2,l} a_{2,l}\rangle = \langle a^+_{3,l} a_{3,l}\rangle$, $e_0 = \frac{3h}{2} - 4J_3 A_1 A_2 + 4J_3 \overline{n}_2 A_3$. In the elementary contractions A_2, A_3 the invariance of the initial Hamiltonian with respect to the space reflection was exploited.

After Fourier transformation,

$$a_{p,\kappa} = \frac{1}{\sqrt{N}} \sum_{l=1}^{N} \mathrm{e}^{-il\kappa} a_{p,l},\ a_{p,l} = \frac{1}{\sqrt{N}} \sum_{\kappa} \mathrm{e}^{il\kappa} a_{p,\kappa},$$
$$\kappa = 2\pi m/N,\ m = -\frac{N}{2}+1, \ldots, \frac{N}{2} (\text{for even } N),$$
$$m = -\frac{N-1}{2}, \ldots, \frac{N-1}{2} (\text{for odd } N),$$

the Hamiltonian can be represented in the matrix form

$$H_{xx} = \sum_{\kappa} \sum_{p,q=1}^{3} \mathcal{H}_{p,q}(\kappa) a^+_{p,\kappa} a_{q,\kappa} + N e_0, \quad (20)$$
$$\mathcal{H}_{11}(\kappa) = -h, \mathcal{H}_{22}(\kappa) = \mathcal{H}_{33}(\kappa) = -h - 2A_3 J_3,$$
$$\mathcal{H}_{12}(\kappa) = \mathcal{H}^*_{21}(\kappa) = \frac{1}{2}(J_1 + 2J_3 A_1 + J_3(1 - 2\overline{n}_2)\mathrm{e}^{-i\kappa}),$$
$$\mathcal{H}_{13}(\kappa) = \mathcal{H}^*_{31}(\kappa) = \frac{1}{2}(J_3(1 - 2\overline{n}_2) + (J_1 + 2J_3 A_1)\mathrm{e}^{-i\kappa}),$$
$$\mathcal{H}_{23}(\kappa) = \mathcal{H}_{32}(\kappa) = \frac{1}{2}(J_2 + 4A_2 J_3).$$

This Hamiltonian can be reduced to a diagonal form:

$$H_{xx} = \sum_{p,\kappa} \Lambda_p(\kappa) \eta^+_{p,\kappa} \eta_{p,\kappa} + N e_0, \quad (21)$$

by some unitary transformation $\eta_{p,\kappa} = \sum_{q=1}^{3} u_{p,q}(\kappa) a_{q,\kappa}$ where $u_{p,q}(\kappa)$ is a unitary matrix. Generally, it corresponds to the 3×3 eigenvalue and eigenvector problems. Finally, we approximately presented the model as the free-fermion gas, and its thermodynamic and correlation functions can be calculated straightforwardly. However, the elementary contractions, which are included into the Hamiltonian parameters, are unknown and have to be found self-consistently:

$$\overline{n}_2 = \langle a^+_{2,l} a_{2,l}\rangle = \sum_{\kappa} \sum_{p} |u_{2,p}(\kappa)|^2 \langle \eta^+_{p,\kappa} \eta_{p,\kappa}\rangle,$$
$$A_1 = \langle a^+_{2,l} a_{3,l}\rangle = \sum_{\kappa} \sum_{p} u^*_{2,p}(\kappa) u_{3,p}(\kappa) \langle \eta^+_{p,\kappa} \eta_{p,\kappa}\rangle,$$
$$A_2 = \langle a^+_{1,l} a_{2,l}\rangle = \sum_{\kappa} \sum_{p} u^*_{1,p}(\kappa) u_{2,p}(\kappa) \langle \eta^+_{p,\kappa} \eta_{p,\kappa}\rangle,$$
$$A_3 = \langle a^+_{1,l} a_{3,l}\rangle = \sum_{\kappa} \sum_{p} u^*_{1,p}(\kappa) u_{3,p}(\kappa) \langle \eta^+_{p,\kappa} \eta_{p,\kappa}\rangle. \quad (22)$$

Here $\langle \ldots \rangle$ means the thermodynamic average with the Hamiltonian (21), and for the ideal Fermi gas $\langle \eta^+_{p,\kappa} \eta_{p,\kappa}\rangle = 1/(\exp(\beta \Lambda_p(\kappa)) + 1)$ is the Fermi function. Thus, the initial statistical mechanical problem for the spin model is turned into the solution of the set of equations (22). We have solved this problem numerically and then used the formulae for the free-fermion gas to calculate the thermodynamics and static properties of the model. Particularly, the equation (14) can be used for calculating the total magnetization.

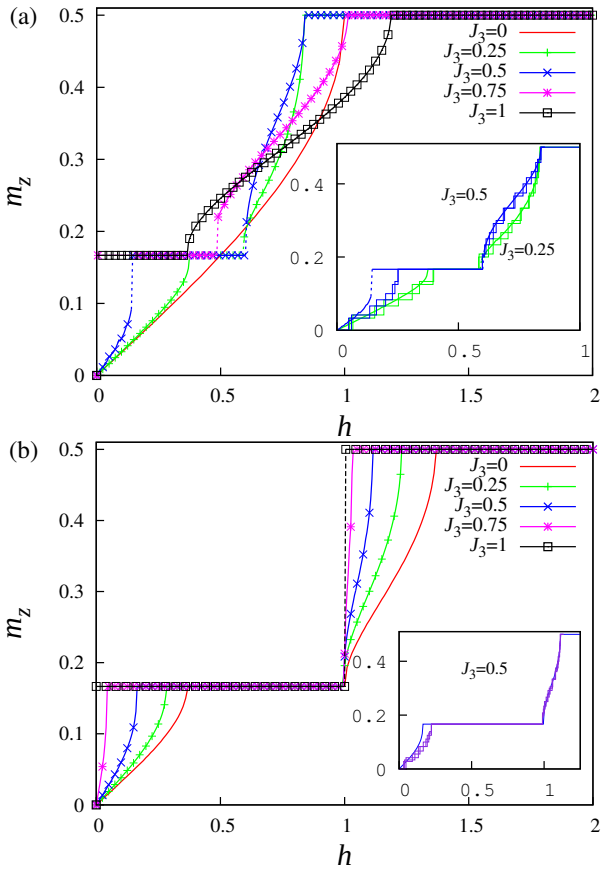

Fig. 3. (Color online) The ground-state magnetization vs. the external field of the distorted diamond chain for $J_1 = 1$, $J_3 = 0, 0.25, 0.5, 0.75, 1$. a) $J_2 = 1$. Inset shows the comparison of the results of the Hartree-Fock approximation and exact diagonalization for $N = 24, 30, 36$ (step-like lines) for $J_3 = 0.25, 0.5$. b) $J_2 = 2$. Inset shows the comparison of the results of the Hartree-Fock approximation and exact diagonalization for $N = 24, 30, 36$ (step-like lines) for $J_3 = 0.5$.

For $T = 0$ $\langle \eta^+_{p,\kappa} \eta_{p,\kappa}\rangle$ becomes the Heaviside step function and the summation in (22) can be restricted to κs which satisfy $\Lambda_p(\kappa) \leq 0$. This simplifies the calculation of the ground state properties of the model. The results for the ground state magnetization are shown in Fig. 3. It is worthwhile to remark that one recovers the exact result for the magnetization curve of the uniform [37,38] and trimerized [40,41] spin-$\frac{1}{2}$ XX chains in the particular cases $J_1 = J_2 = 1$, $J_3 = 0$ and $J_1 = 1$, $J_2 = 2$, $J_3 = 0$ shown in Fig. 3. Another particular case, which is amenable for an exact calculation, is the dimer-monomer limit $J_2 = 2$, $J_1 = J_3 = 1$ (see Fig. 3b). The magnetization has a step-like shape in this special case (see Appendix). The Hartree-Fock equations (22) have the following solu-

tions for the elementary contractions: $\overline{n}_2 = \frac{1}{2}$, $A_1 = -\frac{1}{2}$, $A_2 = A_3 = 0$ for $h < \frac{J_2}{2}$. Inserting the solutions obtained for $J_2 = 2$, $J_1 = J_3 = 1$ into Eq. (19), one comes to the approximative Hamiltonian in the form

$$H_{xx} = \frac{1}{2}\sum_{l=1}^{N}\Bigg[J_2(c^+_{2,l}c_{3,l} + c^+_{3,l}c_{2,l}) - 2h\left(c^+_{1,l}c_{1,l} + c^+_{2,l}c_{2,l} + c^+_{3,l}c_{3,l} - \frac{3}{2}\right)\Bigg]. \quad (23)$$

It can be diagonalized by the canonical transformation: $\eta_{s,l} = \frac{1}{\sqrt{2}}(c_{2,l} - c_{3,l})$, $\eta_{t,l} = \frac{1}{\sqrt{2}}(c_{2,l} + c_{3,l})$, $\eta_{m,l} = c_{1,l}$. As a result we come to the free-fermion gas of the form:

$$H_{xx} = \frac{1}{2}\sum_{l=1}^{N}\Bigg[J_2(\eta^+_{t,l}\eta_{t,l} - \eta^+_{s,l}\eta_{s,l}) - 2h\left(\eta^+_{t,l}\eta_{t,l} + \eta^+_{s,l}\eta_{s,l} + \eta^+_{m,l}\eta_{m,l} - \frac{3}{2}\right)\Bigg]. \quad (24)$$

The ground state of the model can be easily found: $|GS\rangle = \prod_l \frac{1}{\sqrt{2}}(c^+_{2,l} - c^+_{3,l})|0\rangle = \prod_l |\downarrow\rangle_{1,l}[2,l;3,l]$ if $h < 0$, $|GS\rangle = \prod_l \frac{1}{\sqrt{2}}c^+_{1,l}(c^+_{2,l} - c^+_{3,l})|0\rangle = \prod_l |\uparrow\rangle_{1,l}[2,l;3,l]$ if $h > 0$. Here $[2,l;3,l]$ represents the singlet dimer state between spins on sites $(2,l)$ and $(3,l)$. As one can see, the Hamiltonian (24) indeed represents the model of non-correlated singlet dimers created between the spins on sites $(2,l)$ and $(3,l)$, which are separated through the free monomeric spins residing the sites $(1,l)$ and thus, there cannot be any correlation between singlet dimers. We note that the same approach also recovers the completely dimerized state in the Majumdar-Ghosh limit of the zig-zag ladder [34].

For the intermediate values of J_3 only approximative results are available. To understand to what extent the elaborated approach is valid we compare it with the results of the exact diagonalization of finite chain up to 36 spins. For some particular values of J_3 such comparison is shown in the insets to Fig. 3. It can be seen that the approximative results are quite accurate for sufficiently strong fields h, and one recovers the 1/3-plateau for the diamond chains. Therefore, the Hartree-Fock method is reliable even for the case of strong frustration ($J_3 \sim J_1$). However, for small field it may produce an artificial jump of the magnetization for $J_3 = 0.25, 0.5, 0.75$ if one compares the results stemming from the Hartree-Fock approach with the data of the exact numerical diagonalization method (see. Fig. 3a).

The comparison with the free-fermion model, see Sect. 3, demonstrates that neglecting of the phase factors leads to quite different magnetization curves. Besides the wrong low-field behavior there is also a significant difference in the saturation field.

The 1/3-plateau in the magnetization curve can be understood from formula (14) as an integral over the density of states. The approximative representation of the initial spin model (1) is a fermionic model with three types of fermions. Thus, the energy spectrum consists of three bands separated by gaps. The external field plays the role of the chemical potential of fermions and thus, it can shift their Fermi level to the area of a gap between two bands. Such a situation corresponds to the 1/3-plateau of the magnetization. It can be also understood that all elementary contractions do not change along the plateau. Therefore, the width of the plateau is equal to the width of the gap in case the magnetization curve does not reveal any jumps.

The effect of J_3 interaction on the ground-state magnetization process can be understood from Fig. 4. We see

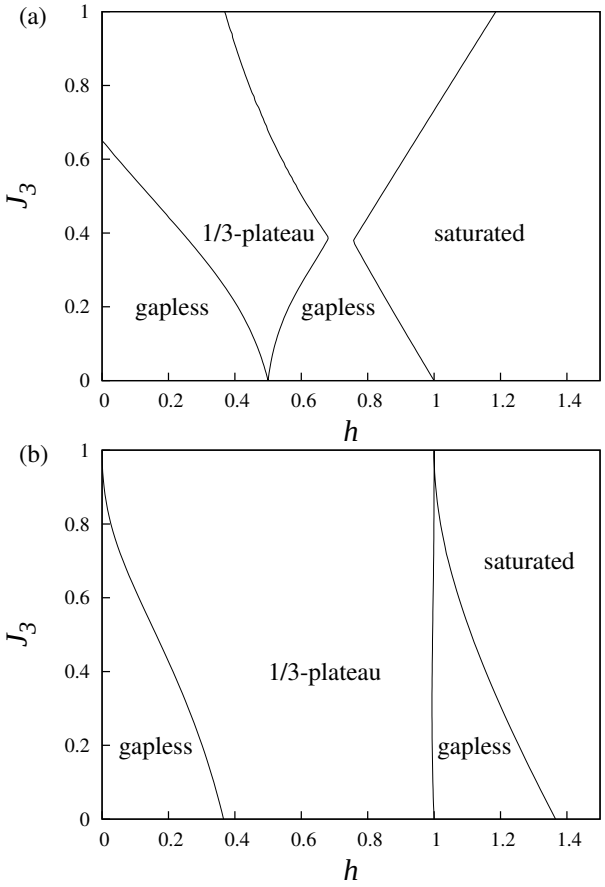

Fig. 4. The ground-state phase diagram of the distorted diamond chain in the Hartree-Fock approximation. The upper (lower) panel corresponds to the case $J_1 = 1$, $J_2 = 1$ ($J_1 = 1$, $J_2 = 2$).

that for initially uniform chain ($J_2 = J_1 = 1$) an addition of the frustrating interaction J_3 generally causes an onset of the intermediate magnetization plateau at $m = 1/3$, which becomes the broader the stronger the interaction parameter J_3 is (see Fig. 4a). Generally, the coupling J_3 increases the width of the magnetization plateau also in case of the initial trimerized chain. It is interesting to note that the upper critical field for the 1/3-magnetization plateau in case $J_1 = 1$, $J_2 = 2$ does not show any marked dependence on J_3.

It should be noted that the ground state phase diagram of the generally anisotropic distorted diamond chain was studied previously [14,15,16]. The so-called inversion areas may be found in this more general model where the Néel phase becomes the ground state in the parameter space with the predominant XY-like interaction and the spin-fluid phase contrary appears in the parameter region with the predominant Ising-like interaction. The Néel order considered in Refs.[14,15,16] is related to the antiferromagnetic ordering of spin blocks $(\mathbf{s}_{3,l-1}+\mathbf{s}_{1,l}+\mathbf{s}_{2,l})$, and thus corresponds to 6 spins in the magnetic cell. This phase seems to disappear in the pure XY limit (see Fig. 2 of Ref.[16]), at least it is true for $J_1 \gg J_2, J_3$. Since we have not considered the possibility of doubling of the elementary magnetic cell in our approach, we cannot verify whether such a phase exists. Moreover, the spin-fluid phase found in Ref. [16] for $h=0$ we do not find in our approach, which might be attributed to its mean-field character.

5 Hartree-Fock approximation for the symmetric diamond chain

Here we consider the case of symmetric diamond chain when the interactions $J_1 = J_3$. For this purpose, let us consider the fermionic representation (9) of the spin Hamiltonian which provides a symmetric representation for those bonds. In the fermionic Hamiltonian we keep all the terms that correspond to the correlation between neighboring sites in the decoupling. Since the coefficients of the Hamiltonian (9) are complex the elementary contractions can also be complex valued. Similarly to previous section we introduce the following notations:

$$\begin{aligned} A_1 &= \langle c^+_{2,l} c_{3,l}\rangle, \\ A_2 &= \langle c^+_{1,l} c_{2,l}\rangle = \langle c^+_{1,l+1} c_{3,l}\rangle, \\ A_3 &= \langle c^+_{1,l} c_{3,l}\rangle = \langle c^+_{1,l+1} c_{2,l}\rangle. \end{aligned} \tag{25}$$

Here we additionally used the invariance of the initial spin Hamiltonian with the respect to the space reflection. The invariance to the exchange of the second and third sublattices, gives us the following connections between different contractions: $A_2 = A_3^*$ ($A_2^R = A_3^R$, $A_2^I = -A_3^I$). Here A_p^R (A_p^I) is the real (imaginary) part of A_p. The Hamiltonian within the adopted approximation will be as follows:

$$\begin{aligned} H_{xx} = \frac{1}{2}\sum_{l=1}^{N} & [J_2 + 4J_1(A_2^R + A_2^I)](c^+_{2,l}c_{3,l} + c^+_{3,l}c_{2,l}) \\ & + \tilde{J}_1^R\left((c^+_{1,l} + c^+_{1,l+1})(c_{2,l} + c_{3,l}) + \text{h.c.}\right) \\ & + i\tilde{J}_1^I\left((c^+_{1,l+1} - c^+_{1,l})(c_{2,l} - c_{3,l}) - \text{h.c.}\right) \\ & - 2(hc^+_{1,l}c_{1,l} + h_2 c^+_{2,l}c_{2,l} + h_2 c^+_{3,l}c_{3,l})] + Ne_0 \end{aligned} \tag{26}$$

where $\tilde{J}_1^R = J_1(1-\overline{n}_2 + A_1^R)$, $\tilde{J}_1^I = J_1(\overline{n}_2 + A_1^R)$, $h_2 = h - 2J_1(A_2^R - A_2^I)$, $e_0 = \frac{3h}{2} - 4J_1A_1^R(A_2^R + A_2^I) + 4J_1n_2(A_2^R - A_2^I)$.

After performing Fourier transformation, the Hamiltonian can be written in a matrix form as follows

$$H_{xx} = \sum_{\kappa}\sum_{p,q=1}^{3} \mathcal{H}_{p,q}(\kappa) a^+_{p,\kappa} a_{q,\kappa} + Ne_0 \tag{27}$$

$$\begin{aligned} &\mathcal{H}_{11}(\kappa) = -h, \\ &\mathcal{H}_{22}(\kappa) = \mathcal{H}_{33}(\kappa) = -h - 2J_1(A_2^R - A_2^I), \\ &\mathcal{H}_{12}(\kappa) = \mathcal{H}^*_{21}(\kappa) = \frac{1}{2}\sqrt{(\tilde{J}_1^R)^2 + (\tilde{J}_1^I)^2}\,(\mathrm{e}^{-i\phi} + \mathrm{e}^{i(\phi-\kappa)}), \\ &\mathcal{H}_{13}(\kappa) = \mathcal{H}^*_{31}(\kappa) = \frac{1}{2}\sqrt{(\tilde{J}_1^R)^2 + (\tilde{J}_1^I)^2}\,(\mathrm{e}^{i\phi} + \mathrm{e}^{-i(\phi+\kappa)}), \\ &\mathcal{H}_{23}(\kappa) = \mathcal{H}_{32}(\kappa) = \frac{1}{2}(J_2 + 4J_1(A_2^R + A_2^I)), \end{aligned} \tag{28}$$

where $\tilde{J}_1 = \sqrt{(\tilde{J}_1^R)^2 + (\tilde{J}_1^I)^2}$, $\tan\phi = \tilde{J}_1^I/\tilde{J}_1^R$.

Similarly to the previous section the problem is rewritten as the free-fermion gas. The Hamiltonian (26) or (27) contains the unknown contractions $\overline{n}_2$, A_1, A_2. These contractions have to be found from the set of self-consistent equations identical to (22).

The results for the ground-state magnetization are presented in Fig. 5. We set $J_1 = 1$ here. One can notice that the magnetization for $J_2 = 2J_1$ corresponds to the exact one (see Appendix). Following the arguments of the previous section, it can be shown that the Hartree-Fock approximation leads to the dimer-monomer ground state which is exact for this case. For $J_2 \geq 2J_1$ the magnetization curve still has a step-like shape and corresponds to the exact result. For intermediate values of J_2 we also obtain rather good coincidence with the exact diagonalization data. We even recover the magnetization jump for intermediate fields which is present also in the exact diagonalization data. However the approximate results for the low-field magnetization show a noticeable difference with the exact diagonalization data. Moreover for $J_2 \gtrsim 0.86J_1$ we get an incorrect non-zero magnetization even for zero fields h. It is well known that if $0.909 < J_2/J_1 < 2$ the singlet dimer-tetramer phase is the ground state of the isotropic diamond chain [7]. This phase survives also in the model with the easy-plane anisotropy [14]. The elementary magnetic cell is doubled in this case. Therefore, the current approach, where a doubling of the unit cell is not taken into account, does not capture this phase. At higher fields the dimer-tetramer order is destroyed and the ordering of the singlet dimers on vertical bonds becomes more favorable (see Fig. 5b). Since the elementary magnetic cell is not doubled anymore, we obtain an excellent agreement between the approximate and exact diagonalization data (see the inset in Fig. 5a). Our exact diagonalization data are also in agreement with the previous results for the easy-plane XXZ diamond chain [14,15,16]. Note that the model with the easy-plane anisotropy in zero field is characterized by the spin-fluid phase for $J_2 \lesssim J_1$ (see Fig. 3 in Ref.[14]) in contrast to the isotropic model where the ferrimagnetic order persists in the ground state [7]. The exact diagonalization data show the continuous growth of the ground-state magnetization with field for $J_2 \lesssim J_1$. This is usually the sign of a gapless excitation spectrum and

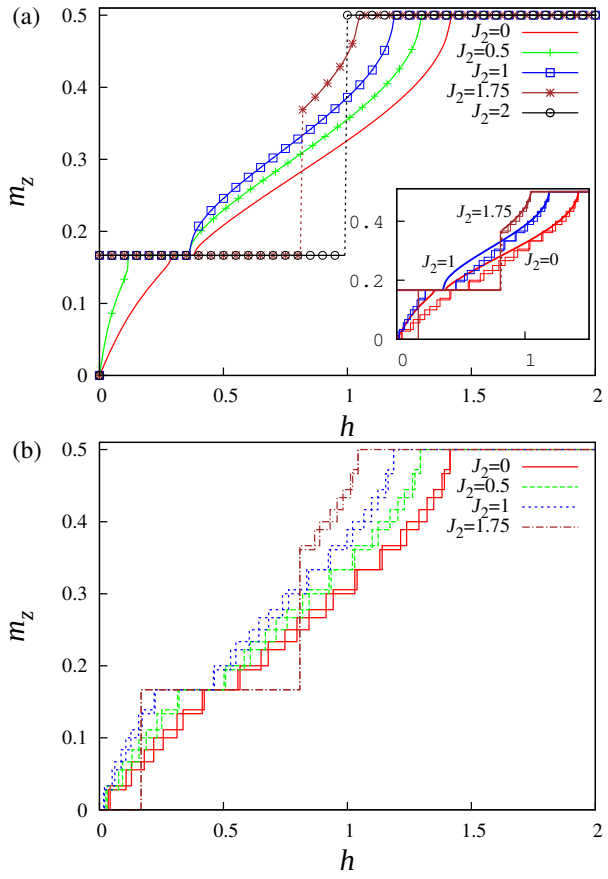

Fig. 5. (Color online) The ground-state magnetization vs. the external field of the symmetric diamond chain: $J_1 = 1$ a) the results for the Hartree-Fock approximation are shown and compared with the exact diagonalization data in the inset for $J_2 = 0, 1, 1.75$; b) the results of the exact diagonalization for finite chains of $N = 30, 36$ spins with $J_2 = 0, 0.5, 1, 1.75$.

the spin-fluid phase. For stronger J_2 couplings we obtain the zero-magnetization plateau and a very steep increase of the magnetization to the 1/3 plateau for some critical field ($h \approx 0.168 J_1$ for $J_2 = 1.75 J_1$). The phase with the zero magnetization plateau can be identified as the singlet dimer-tetramer phase, and critical field as a field which destroys tetramers in the ground state. Considering the ground-state phase diagram presented in Fig. 6, we have to conclude that the considered Hartree-Fock approach is not able to exhibit the singlet dimer-tetramer phase with the zero magnetization plateau which appears in the thin region of small fields and $1 \lesssim J_2/J_1 \leq 2$ in accordance with the exact diagonalization data. However, as soon as the magnetic cell is not doubled anymore, the ground state phase diagram are in good agreement with the exact diagonalization data.

Again, the comparison with the free-fermion model, see Sect. 3, shows that it is not a reasonable approximation to neglect the phase factors. In particular, the jump found within our approach and confirmed by exact diagonalization is not present in the free-fermion model. Comparing the results of the previous section we see that both formulations with different gauges produces the same results for the ground state properties. Thus the Hartree-Fock approximation preserves the gauge invariance.

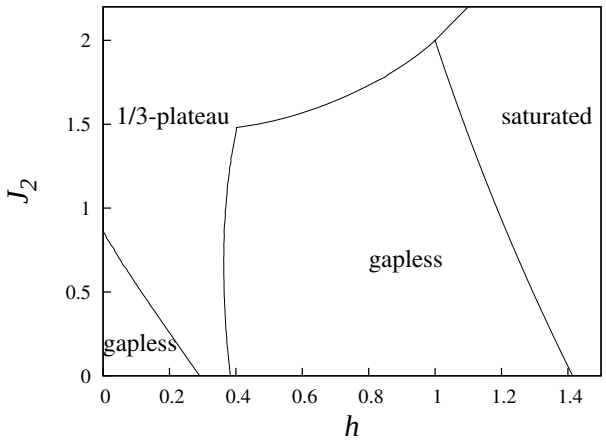

Fig. 6. The ground-state phase diagram in the $h - J_2$ plane for the symmetric diamond chain with $J_1 = J_3 = 1$ in the Hartree-Fock approximation.

The results of the exact diagonalization show also some indication of the second plateau at 2/3 of the saturated magnetization. We note that the elaborated Hartree-Fock approach cannot reproduce such a behavior. To get it one has to consider the possibility of doubling of the elementary magnetic cell in the decoupling procedure which was not assumed in Eqs. (25) and (26).

6 Diamond chain at non-zero temperatures

In this section we consider the thermodynamic properties of the diamond chain within the fermionization approach and the Hartree-Fock approximation. After having rewritten the spin Hamiltonian as a quadratic form of Fermi operators, one can find its eigenvalues and obtain the Helmholtz free energy per site:

$$f = -\frac{1}{3N\beta}\sum_{p=1}^{3}\sum_{\kappa}\ln(\mathrm{e}^{-\beta\Lambda_p(\kappa)}+1)$$
$$= -\frac{1}{\beta}\int_{-\infty}^{\infty} dE\rho(E)\ln(\mathrm{e}^{-\beta E}+1), \qquad (29)$$

the internal energy per site

$$u = \frac{1}{3N}\langle H\rangle = \int_{-\infty}^{\infty} dE\rho(E)n(E)E + e_0, \qquad (30)$$

and the specific heat per site $c = \frac{du}{dT}$

$$c = \frac{1}{T^2}\int_{-\infty}^{\infty} dE\rho(E)n^2(E)E^2\mathrm{e}^{\beta E} + \frac{\partial u}{\partial \overline{n_2}}\frac{\partial \overline{n_2}}{\partial T} + \sum_{p=1}^{3}\frac{\partial u}{\partial A_p}\frac{\partial A_p}{\partial T}. \qquad (31)$$

Here $\beta = 1/T$ is the inverse temperature.

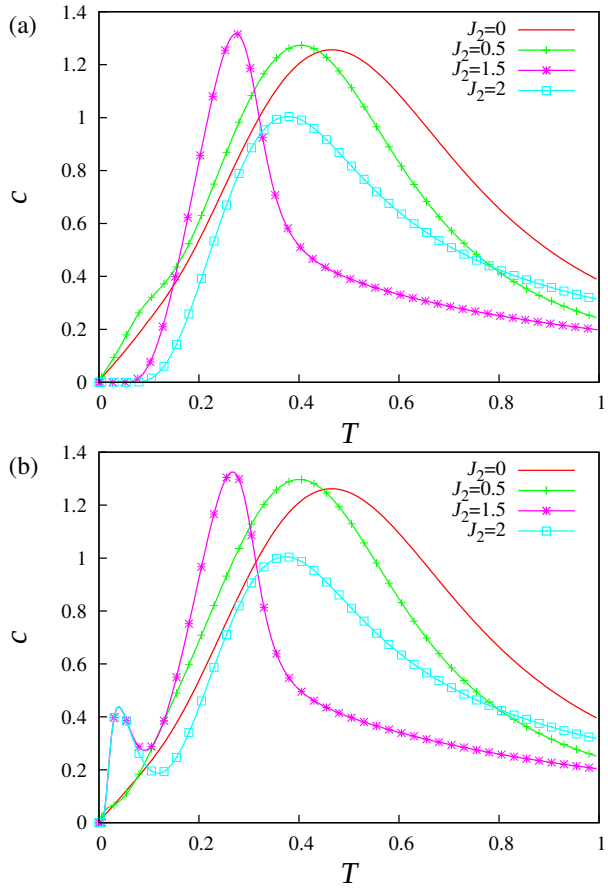

Fig. 7. (Color online) The specific heat in the Hartree-Fock approximation vs. temperature of the symmetric diamond chain ($J_1 = J_3 = 1$), $J_2 = 0, 0.5, 1.5, 2$: a) $h = 0$, b) $h = 0.1$.

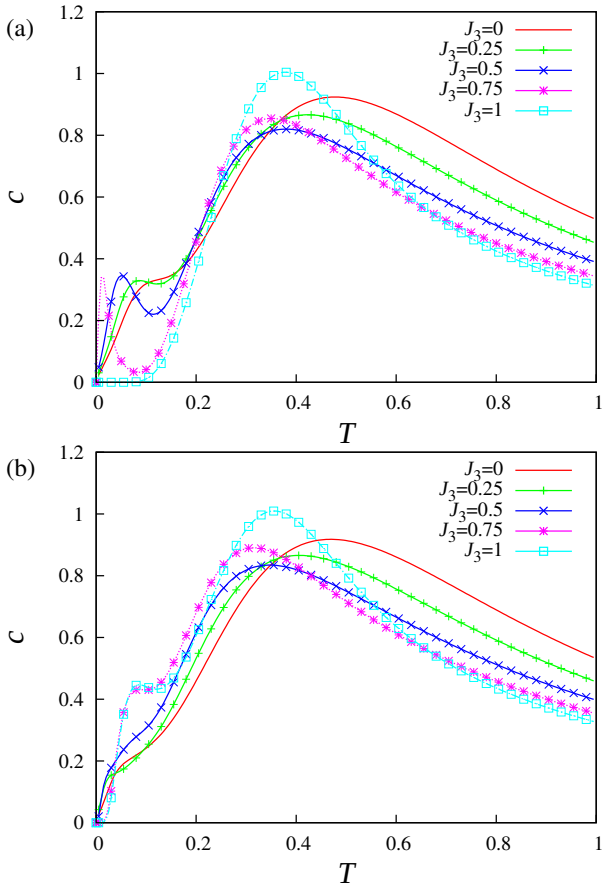

Fig. 8. (Color online) The specific heat in the Hartree-Fock approximation vs. temperature of the distorted diamond chain $J_1 = 1$, $J_2 = 2$, $J_3 = 0, 0.25, 0.5, 0.75, 1$: a) $h = 0$, b) $h = 0.2$.

To calculate the specific heat we perform the numerical differentiation. The results of computations are shown in Figs. 7 and 8. Some typical features can be observed there. The specific heat for small vertical couplings J_2 grows up linearly with the temperature which is inherent for systems with a gapless excitation spectrum. For sufficiently strong J_2 (see the curves corresponding to $J_2 = 1.5, 2$ in Fig. 7) the ground state is degenerate due to dimer-monomer phase, and the system has a gap between the ground and excited states. Therefore, we observe the exponential growth of the specific heat with temperature. When a small external field h is applied, it does not produce a gap in the excitation spectrum, thus the temperature dependence of the specific heat remains qualitatively the same. The effect of the external field on the dimer-monomer phase is somewhat different. The ground state degeneracy is lifted due to the Zeeman term $-h\sum_{p,l} s^z_{p,l}$. As a results we have two kinds of excitations with different gaps. This leads to the appearance of the double-peak structure in the temperature dependence of the specific heat. The first peak corresponds to the low-energy flip excitations of the monomer spins $s_{1,l}$, and the second one corresponds to the thermal excitations of the spins creating singlet dimers. Here we should emphasize that the dimer-monomer phase as well as the ground state degeneracy is an artifact of the elaborated approximation for $0.909 < J_2/J_1 < 2$ (see discussion in Sec. 5). Therefore, the results presented in Fig. 7 for $J_2 = 1.5$ cannot reproduce the features of the specific heat of the spin-$\frac{1}{2}$ XX diamond chain.

In contrast to the symmetric chain, the distorted diamond chain shows the double-peak structure in the temperature dependence of the specific heat even in the zero-field case (see Fig. 8), whereas the external field can even demolish this double-peak structure. The mentioned features are not only the consequence of the XX anisotropy in the spin interaction. The similar behavior of the temperature dependent specific heat with the double-peak structure was also reported for the Heisenberg diamond chain, see Fig. 8 of Ref. [30]. The external field can also lead to less visible double-peak structure in the specific heat of the Heisenberg diamond chain [48].

The field dependent magnetization for non-zero temperatures can be also understood. The plateaux and jumps of the magnetization are smeared out by temperature (see Fig. 9). One exception is the model when $J_2 \sim J_1$ when the mean-field treatment preserves jumps even for small temperatures. Thus, the Hartree-Fock approximation turns

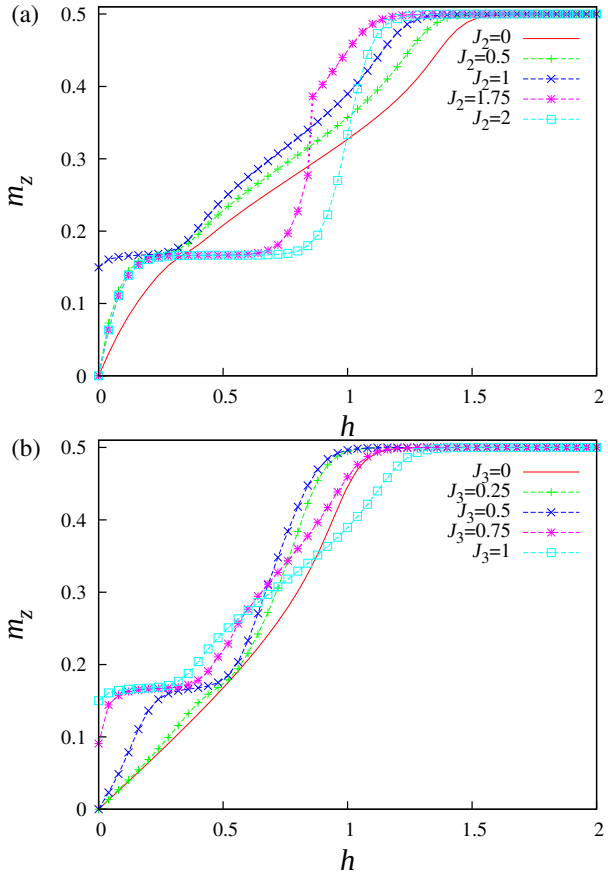

Fig. 9. (Color online) The magnetization in the Hartree-Fock approximation vs. the external field of the diamond chain for $T = 0.05J_1$: a) $J_1 = J_3 = 1$, $J_2 = 0, 0.5, 1, 1.75, 2$; b) $J_1 = J_2 = 1$, $J_3 = 0, 0.25, 0.5, 0.75, 1$

out to be incorrect for $J_1 \sim J_2 \sim J_3$ and small external field h, since the spontaneous (i.e. non-zero) magnetization in the zero-field limit is prohibited for one-dimensional system at any finite temperature due to the Mermin-Wagner theorem [49].

7 Conclusions

In the present work, we consider the Jordan-Wigner transformation for the spin-$\frac{1}{2}$ XX model on the diamond chain by assuming a quite general distorted case.

At first we showed that the free-fermion model on the diamond chain cannot describe the spin system since it loses the symmetries of a spin model and exhibits a non-zero magnetization in zero magnetic field. In the case of the distorted chain we apply the Hartree-Fock approximation for the fermionic representation of the model which considers the fermion interaction along weaker bonds. For the symmetric diamond chain we suggest the generalization of the Jordan-Wigner transformation and build a fully symmetric fermionic representation of the spin-model. Further, we use the Hartree-Fock approximation to study the model near the limit of the dimer-monomer phase when the correlation between the spins from the vertical bonds are the strongest one. The Hartree-Fock approximation reproduces an exact result for the dimer-monomer ground state of the symmetric diamond chain ($J_2 \geq 2J_1$). Moreover, we have found that the solutions of the Hartree-Fock approximation for the symmetric diamond chain are invariant with respect to the gauge transformations. Our results show also good agreement with the exact diagonalization data reproducing the magnetic properties at high fields or small frustrations. Summarizing our findings, the elaborated approach for the XX diamond chain reproduces a plateau in the magnetization curve at 1/3 of the saturation magnetization and an additional peak in the specific heat curve. In fermionic language a 1/3 plateau is caused by the gap between two fermionic bands. When the gap becomes large enough, the temperature dependence of the specific heat gains a distinct two-peak structure. Note that both features are typical for azurite [23, 25, 26, 27] although the Heisenberg model seems to be more appropriate for that compound.

We have also observed some drawbacks of the Hartree-Fock treatment. It becomes invalid for $J_1 \sim J_2 \sim J_3$. In this case mean-fields leads to the non-zero magnetization in zero fields, and the magnetization jump survives also for small temperatures.

The authors would like to thank O. Derzhko for the useful discussions. T.V. was supported by the National Scholarship Programme of the Slovak Republic. J.S. and M.J. acknowledge the financial support by the ERDF EU (European Union European regional development fund) grant provided under the contract No. ITMS26220120005 (activity 3.2.).

Appendix: Exact monomer-dimer ground state for the anisotropic diamond chain

In case $J_1 = J_3 > 0$ and $J_2 \geq 2J_1$ the ground state of the Hamiltonian on the diamond chain is the dimer-monomer state [7]. To prove this we can follow the arguments of Shastry and Sutherland to obtain the ground state [47]. We have to consider the Hamiltonian as a sum of Hamiltonians of triangles:

$$
\begin{aligned}
H &= \sum_l H_{l,l} + H_{l,l+1}, \\
H_{l,l} &= \frac{J_2}{2}(\mathbf{s}_{2,l} \cdot \mathbf{s}_{3,l})_\Delta + J_1 \left((\mathbf{s}_{1,l} \cdot \mathbf{s}_{2,l})_\Delta \right. \\
&\quad \left. +(\mathbf{s}_{1,l} \cdot \mathbf{s}_{3,l})_\Delta\right) - \frac{h}{2}\left(s^z_{1,l} + s^z_{2,l} + s^z_{3,l}\right), \\
H_{l,l+1} &= \frac{J_2}{2}(\mathbf{s}_{2,l} \cdot \mathbf{s}_{3,l})_\Delta + J_1 \left((\mathbf{s}_{1,l+1} \cdot \mathbf{s}_{2,l})_\Delta \right. \\
&\quad \left. +(\mathbf{s}_{1,l+1} \cdot \mathbf{s}_{3,l})_\Delta\right) - \frac{h}{2}\left(s^z_{1,l+1} + s^z_{2,l} + s^z_{3,l}\right).
\end{aligned}
$$

Here we introduced the notation $(\mathbf{s}_{p,l} \cdot \mathbf{s}_{q,m})_\Delta = s^x_{p,l}s^x_{q,m} + s^y_{p,l}s^y_{q,m} + \Delta s^z_{p,l}s^z_{q,m}$. The parts of the systems described by $H_{l,l}$ and $H_{l,l+1}$ are topologically identical. Therefore,

they have the same eigenvalues and analogous eigenstates. One can use the variational principle that implies $E_0 \geq N(e_l + e_l)$, where e_l is the ground state energy of $H_{l,l}$ or $H_{l,l+1}$.

Let us consider the case $J_2 > 2J_1$. The direct calculation shows that if $|h| \leq h_c = \frac{\Delta(J_2+2J_1)+J_2}{2}$ the dimer-monomer state $|\alpha_{1,l}\rangle[2l, 3l]$ of $H_{l,l}$ or $H_{l,l+1}$ is the state with the lowest eigenvalue $e_l^{dm} = -\frac{(\Delta+2)J_2}{8} - \frac{|h|}{4}$ and $S^z_{tot} = \pm\frac{1}{2}$. Here $|\alpha_{1,l}\rangle$ denotes the spin up state $|\uparrow_{1,l}\rangle$ if $h > 0$, or the spin down state $|\downarrow_{1,l}\rangle$ if $h < 0$. Thus using the variational principle the ground state of the whole crystal can be built by translation of the state $|\alpha_{1,l}\rangle[2l, 3l]$ over all sites. The total magnetization is $\frac{N}{2}\mathrm{sgn}(h)$ and the magnetization per spin is 1/6. Contrary, if $|h| > h_c$, the completely polarized state with $S^z_{tot} = \pm\frac{3}{2}$ becomes the state with the lowest eigenvalue $e_l^{3/2} = \frac{\Delta(J_2+4J_1)}{8} - \frac{3|h|}{4}$. Thus, the total ground state is the state with all spins up or down, with the magnetization per spin $m^z = 1/2$.

To summarize, the field dependence of the ground-state magnetization has a step-like form for $J_2 > 2J_1$, i.e., $m^z = \mathrm{sgn}(h)/6$ if $|h| < h_c$ and $m^z = \mathrm{sign}(h)/2$ otherwise, whereas the critical field equals to $h_c = J_1\Delta + J_2(1+\Delta)/2$.

References

1. G. Misguich, C. Lhuillier, in: Frustrated Spin Systems, edited by H.T. Diep, (World Scientific, Singapore, 2004), p.229
2. H.-J. Mikeska, A.K. Kolezhuk, in: Quantum Magnetism, edited by U. Schollwöck, J. Richter, D.J.J. Farnell, R.F. Bishop, Lect. Notes Phys. **645**, (Springer, Berlin, 2004), p.1
3. J. Richter, J. Schulenburg, A. Honecker, edited by U. Schollwöck, J. Richter, D.J.J. Farnell, R.F. Bishop, Lect. Notes Phys. **645**, (Springer, Berlin, 2004), p.85
4. O. Derzhko, J. Richter, A. Honecker, H.-J. Schmidt, Fizika Nizkikh Temperatur **33**, 982 (2007) [Low Temp. Phys. **33**, 745 (2007)]
5. J. Schulenburg, A. Honecker, J. Schnack, J. Richter, H.-J. Schmidt, Phys. Rev. Lett. **88**, 167207 (2002)
6. A. Honecker, J. Schulenburg, J. Richter, J. Phys.: Condens. Matter **16**, S749 (2004)
7. K. Takano, K. Kubo, H. Sakamoto, J. Phys.: Condens. Matter **8**, 6405 (1996)
8. L. Čanová, J. Strečka, M. Jaščur, J. Phys.: Condens. Matter **18**, 4967 (2006)
9. K. Takano, H. Suzuki, K. Hida, Phys. Rev. B **80**, 104410 (2009)
10. K. Hida, K. Takano, H. Suzuki, J. Phys. Soc. Jpn. **78**, 084716 (2009)
11. K. Hida, K. Takano, H. Suzuki, J. Phys. Soc. Jpn. **79**, 044702 (2010)
12. K. Okamoto, T. Tonegawa, Yu. Takahashi, M. Kaburagi, J. Phys.: Condens. Matter **11**, 10485 (1999)
13. K. Okamoto, T. Tonegawa, M. Kaburagi, J. Phys.: Condens. Matter **15**, 5979 (2003)
14. K. Okamoto, A. Tokuno, Y. Ichikawa, J. Phys. Chem. Solids **66**, 1442 (2005)
15. A. Tokuno, K. Okamoto, J. Phys. Soc. Jpn. Suppl. **74**, 157 (2005)
16. K. Okamoto, A. Tokuno, T. Sakai, J. Magn. Magn. Mater., **310**, e457-e459 (2007)
17. H. Kikuchi, Y. Fujii, M. Chiba, S. Mitsudo, T. Idehara, Physica B **329-333** 967 (2003)
18. Y. Hosokoshi, K. Katoh, Y. Nakazawa, H. Nakano, K. Inoue, J. Am. Chem. Soc. **123**, 7921 (2001)
19. H. Sakurai, K. Yoshimura, K. Kosuge N. Tsujii, H. Abe, H. Kitazawa, G. Kido, H. Michor, G. Hilscher, J. Phys. Soc. Jpn. **71**, 1161 (2002)
20. D. Uematsu, M. Sato, J. Phys. Soc. Jpn. **76**, 084712 (2007)
21. G. Lazari, T. C. Stamatatos, C. P. Raptopoulou V. Psycharis, M. Pissas, S.P. Perlepes, A.K. Boudalis, Dalton Trans. 3215 (2009)
22. H. Ohta, S. Okubo, T. Kamikawa *et al.*, J. Phys. Soc. Jpn. **72**, 2464 (2003)
23. H. Kikuchi, Y. Fujii, M. Chiba *et al.*, J. Magn. Magn. Mater. **272-276**, 900 (2004)
24. H. Ohta, S. Okubo, Y. Inagaki *et al.*, Physica B **346-347**, 38 (2004)
25. H. Kikuchi, Y. Fujii, M. Chiba *et al.*, Progr. Theor. Phys. Suppl. **159**, 1 (2005)
26. H. Kikuchi, Y. Fujii, M. Chiba, S. Mitsudo, T. Idehara, T. Tonegawa, K. Okamoto, T. Sakai, T. Kuwai, H. Ohta, Phys. Rev. Lett. **94**, 227201 (2005)
27. K.C. Rule, A.U.B. Wolter, S. Sullow, D.A. Tennant, A. Bruhl, S. Kohler, B. Wolf, M. Lang, J. Schreuer, Phys. Rev. Lett. **100**, 117202 (2008)
28. H.-J. Mikeska, C. Luckmann, Phys. Rev. B **77**, 054405 (2008)
29. H. H. Fu, K. L. Yao, Z. L. Liu, Phys. Rev. B **73**, 104454 (2006); Phys. Rev. B **77**, 219901(E) (2008)
30. B. Gu, G. Su, Phys. Rev. B **75**, 174437 (2007)
31. H. Jeschke, I. Opahle, H. Kandpal, *et al.*, arXiv:1012.1090v1 [cond-mat.str-el]
32. M. Azzouz, Liang Chen, S. Moukouri, Phys. Rev. B **50**, 6233 (1994)
33. T. S. Nunner, Th. Kopp, Phys. Rev. B **69**, 104419 (2004)
34. T. Verkholyak, A. Honecker, W. Brenig, Eur. Phys. J. B. **49**, 283 (2006)
35. G. Müller, H. Thomas, H. Beck, J. C. Bonner, Phys. Rev. B **24**, 1429 (1981)
36. O. Derzhko, T. Krokhmalskii, J. Stolze, G. Müller, Phys. Rev. B **71**, 104432 (2005)
37. E. Lieb, T. Schultz, D. Mattis, Ann. Phys. (N.Y.) **16**, 407 (1961)
38. S. Katsura, Phys. Rev. **127**, 1508 (1962); **129**, 2835 (1963)
39. C. E. Zaspel, J. Chem. Phys. **86**, 4713 (1987)
40. K. Okamoto, Solid State Commun. **83**, 1039 (1992)
41. K. Okamoto, Solid State Commun. **98**, 245 (1996)
42. O. Derzhko, J. Richter, V. Derzhko, Ann.Phys. (Leipzig) **8**, SI-49 (1999); cond-mat/9908425v1
43. K. Elk, W. Gasser, Die Methode der Greenschen Funktionen in der Festkörperphysik, (Akademie-Verlag, Berlin, 1979)
44. D.V. Dmitriev, V.Y. Krivnov, A.A. Ovchinnikov, Phys. Rev. B **65**, 172409 (2002)
45. J.-S. Caux, F. H. L. Essler, U. Löw, Phys. Rev. B **68**, 134431 (2003)
46. R. Hagemans, J.-S. Caux, U. Löw, Phys. Rev. B **71**, 014437 (2005)
47. B. S. Shastry, B. Sutherland, Physica B **108**, 1069 (1981); Phys. Rev. Lett. **47**, 964 (1981)
48. Yan-Chao Li, J. Appl. Phys. **102**, 113907 (2007)
49. N. D. Mermin, H. Wagner, Phys. Rev. Lett. **17**, 1133 (1966)